

# A study on compressive strength of concrete in flexural regions of reinforced concrete beams using finite element analysis

Chang-Geun Cho<sup>†</sup>

Research Institute for Disaster Prevention, Kyungpook National University,  
Sankyuk-Dong 1370, Puk-Ku, Taegu, Korea

Hisato Hotta<sup>‡</sup>

Department of Architecture and Building Engineering, Tokyo Institute of Technology,  
Ookayama 2-12-1, Meguro-Ku, Tokyo, Japan

**Abstract.** Based on the orthotropic hypoelasticity formulation, a triaxial constitutive model of concrete is proposed. To account for increasing ductility in high confinement of concrete, the ductility enhancement is considered using so called the strain enhancement factor. It is also developed a three-dimensional finite element model for reinforced concrete structural members based on the proposed constitutive law of concrete with the smeared crack approach. The concrete confinement effects due to the beam-column joint are investigated through numerical examples for simple beam and structural beam member. Concrete at compression fibers in the vicinity of beam-column joint behaves dominant not only by the uniaxial compressive state but also by the biaxial and triaxial compressive states. For the reason of the severe confinement of concrete in the beam-column joint, the flexural critical cross-section is observed at a small distance away from the beam-column joint. These observations should be utilized for the economic design when the concrete structural members are subjected to high confinement due to the influence of beam-column joint.

**Key words:** compressive strength of concrete; hypoelastic model; finite element analysis; concrete confinement due to beam-column joint.

---

## 1. Introduction

In the design of reinforced concrete structural members, the uniaxial compressive strength of concrete obtained from cylinder test is one of the most important design variables as the compressive strength criteria of concrete. In ACI design standard (1999) or in the case of cross-sectional analysis using equivalent rectangular stress block theory (Hognestad *et al.* 1955) or in a fiber model (Kaba *et al.* 1984), generally, it is considered that concrete at compression fibers in structural member is only in a uniaxial compressive state except the confinement effect by transverse reinforcement. However, it is well known that the compressive strength of concrete is

---

<sup>†</sup> Researcher and Lecturer

<sup>‡</sup> Associate Professor

highly dependent on existing various confinement effects, and the axial compressive strength of concrete is increased with the increment of hydrostatic pressure. Under very high confining stresses, extremely high compressive strengths have been recorded. It gives a question that the stress state can be different with uniaxial stress state in flexural critical cross-section of concrete members. It is because the flexural critical region of member, in general, exists near the beam-column joints as shown in Fig. 1, and concrete in that region can be confined by beam-column joint. As shown in the figure, concrete at point A in a simple beam is expected to behave as the uniaxial compressive state, but concrete at point B in a structural member is expected to behave as the multiaxial compressive state. From a previous study on compressive strength of concrete prism with several height/width ratios by Hotta and Cho (1999), it was known that the compressive strength of concrete prism was highly dependent on the restraint effect according with several height/width ratios of specimen. Takiguchi, *et al.* (1992, 1994, 1995, 1996) conducted a series of experimental tests of reinforced concrete beam-column members under several loading conditions and it was to make clear that the characteristic of the compressive strength of concrete was inconstant in the critical section of the members according with the various loading and topology conditions.

The purpose of this study is to investigate the compressive strength of concrete in the vicinity of the flexural critical regions of reinforced concrete structural beam and column members using three-dimensional finite element models. In the experiments of reinforced concrete members, it is difficult to measure the actual triaxial stresses in concrete. The nonlinear finite element analysis of reinforced concrete members with a triaxial constitutive law of concrete can give not only abundant information on the triaxial stress state of concrete, but also easily understanding about confining effect on the compressive strength of concrete in members. Due to that, it is developed a triaxial constitutive law of concrete based on the orthotropic hypoelasticity model for three-dimensional finite element formulation and the validation studies for numerical results have been presented to compare with the experimental results. Using developed finite element model, concrete confinement effects to the flexural strength of reinforced concrete beam member in the beam-column joint have been studied mainly based on the observation of numerical results, with limiting to the case of no

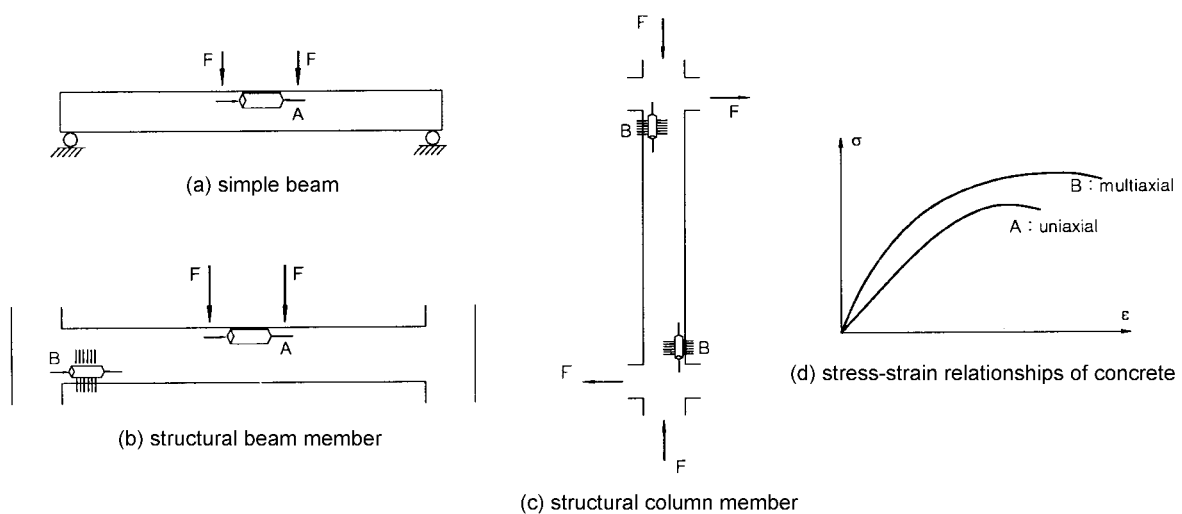


Fig. 1 Compressive stress states of concrete in flexural critical regions

transverse shear reinforcement. These observations give some benefits that there will be actually economies in design practice for structural beam members resulting from concrete confinement due to the influence of beam-column joint.

## 2. Concrete model in compression

The presented three-dimensional stress-strain relationship of concrete is based on an orthotropic hypoelastic formulation with a stress-equivalent uniaxial strain relation. It includes the effects of triaxial nonlinear stress-strain behavior, dilatancy, and the compressive crushing of concrete.

### 2.1 Orthotropic hypoelastic formulation

In structures where the stress state at every point is defined by three principal stresses, concrete can be characterized during loading as a nonlinear orthotropic medium with the directions of orthotropy coincident with the principal stress directions. In this approach, the incremental stress-strain relations of concrete in multiaxial stress state for an orthotropically anisotropic material, as developed by Elwi and Murray (1979) for concrete under axisymmetric stress conditions, can be written as

$$\{d\sigma\} = [C]\{d\varepsilon\} \tag{1}$$

where  $\{d\sigma\}$  and  $\{d\varepsilon\}$  are the vector of stress and strain increments, respectively,  $[C]$  is the constitutive matrix. The following constraints must be fulfilled to ensure the symmetric condition of the compliance tensor:

$$v_{12}E_1 = v_{21}E_2, v_{13}E_1 = v_{31}E_3, v_{23}E_3 = v_{32}E_3 \tag{2}$$

By incorporating the above conditions, consequently, the incremental stress-strain relationship of concrete in the local coordinate system of axes (1, 2, and 3) in the explicitly symmetric form is

$$\begin{Bmatrix} d\sigma_1 \\ d\sigma_2 \\ d\sigma_3 \\ d\tau_{12} \\ d\tau_{23} \\ d\tau_{31} \end{Bmatrix} = \frac{1}{\Omega} \begin{bmatrix} C_{11} & C_{12} & C_{13} & 0 & 0 & 0 \\ & C_{22} & C_{23} & 0 & 0 & 0 \\ & & C_{33} & 0 & 0 & 0 \\ & & & G_{12} & 0 & 0 \\ Sym. & & & & G_{23} & 0 \\ & & & & & G_{31} \end{bmatrix} \begin{Bmatrix} d\varepsilon_1 \\ d\varepsilon_2 \\ d\varepsilon_3 \\ d\gamma_{12} \\ d\gamma_{23} \\ d\gamma_{31} \end{Bmatrix} \tag{3}$$

where

$$C_{11} = E_1(1 - \mu_{32}^2), C_{22} = E_2(1 - \mu_{13}^2), C_{33} = E_3(1 - \mu_{12}^2) \tag{4}$$

$$C_{12} = \sqrt{E_1 E_2}(\mu_{13}\mu_{32} + \mu_{12}), C_{13} = \sqrt{E_1 E_3}(\mu_{12}\mu_{32} + \mu_{13}) \tag{5}$$

$$C_{23} = \sqrt{E_2 E_3}(\mu_{21}\mu_{31} + \mu_{23}), \mu_{ij}^2 = v_{ij}v_{ji} \tag{6}$$

$$\Omega = 1 - \mu_{12}^2 - \mu_{23}^2 - \mu_{31}^2 - 2\mu_{12}\mu_{23}\mu_{31} \tag{7}$$

and the subscripts 1, 2, and 3 stand for the axes of orthotropy;  $\varepsilon$  and  $\gamma$  are normal and engineering shear strains, respectively;  $E_i$  is the tangential modulus of elasticity with respect to the orthotropic direction  $i$  ( $i = 1, 2, 3$ );  $\nu_{ij}$  is the Poisson's ratio in direction  $i$  due to uniaxial stress in direction  $j$  ( $i, j = 1, 2, 3$ ); and  $G_{ij}$  is the shear modulus of elasticity in plane  $i$ - $j$  which is assumed to be invariant with respect to transformation to any non-orthotropic set of axes which results in:

$$G_{12} = [E_1 + E_2 - 2\mu_{12}\sqrt{E_1E_2} - (\sqrt{E_1}\mu_{23} + \sqrt{E_2}\mu_{31})^2]/4 \tag{8}$$

$$G_{23} = [E_2 + E_3 - 2\mu_{23}\sqrt{E_2E_3} - (\sqrt{E_2}\mu_{31} + \sqrt{E_3}\mu_{12})^2]/4 \tag{9}$$

$$G_{31} = [E_3 + E_1 - 2\mu_{31}\sqrt{E_3E_1} - (\sqrt{E_3}\mu_{12} + \sqrt{E_1}\mu_{23})^2]/4 \tag{10}$$

### 2.2 Equivalent uniaxial strains

For the incremental stress-strain relation in Eq. (3), it is necessary to describe the determination of the nine incremental moduli. To this end, the concept of equivalent uniaxial strain, as proposed by Darwin *et al.* (1977), is adopted in the material model. By the transformation of Eq. (3), the equivalent uniaxial strains  $d\varepsilon_{ui}$  can be expressed in terms of the actual incremental strains  $d\varepsilon_i$  as

$$d\varepsilon_{ui} = B_{i1}d\varepsilon_1 + B_{i2}d\varepsilon_2 + B_{i3}d\varepsilon_3, \quad B_{ij} = \frac{C_{ij}}{E_i} \tag{11}$$

The equivalent uniaxial strain increments can be evaluated from Eq. (3) and Eq. (11) in simple form

$$d\varepsilon_{ui} = \frac{d\sigma_i}{E_i} \tag{12}$$

Eq. (12) shows that the equivalent uniaxial strain increment represents the strain increment in the  $i$ -direction that the material would exhibit under a uniaxial stress increment with the other stresses kept equal to zero.

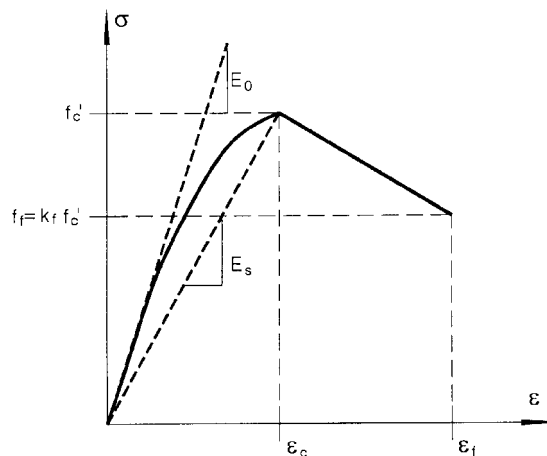


Fig. 2 Uniaxial stress-strain curve of concrete

### 2.3 Uniaxial stress-strain curve and Poisson's ratio

For the uniaxial compressive stress-strain relationship of concrete, as shown in Fig. 2, Saenz (1964)'s curve is adopted to describe the compressive ascending region of concrete. In the compressive descending region of concrete, stress is reduced linearly, and concrete is crushed if any point reaches at ultimate stress,  $f_c$ . On the other hand, a significant volumetric expansion of concrete subjected to higher strains has been observed during experiments. Based on results reported by Kupfer *et al.* (1973) the following equations are used to describe the variation of Poisson's ratio.

$$\nu = \nu_o \left[ 1 + \left( 4 - 5 \frac{\epsilon}{\epsilon_c} \right)^2 \right], \quad \text{for } \epsilon_c \leq \epsilon < 0.8 \epsilon_c \quad (13)$$

$$\nu = \min \left[ \nu_o \left( 3 \frac{\epsilon}{\epsilon_c} + 2 \frac{\epsilon_f}{\epsilon_c} - 5 \right) / \left( \frac{\epsilon_f}{\epsilon_c} - 1 \right), 0.5 \right], \quad \text{for } \epsilon_f \leq \epsilon < \epsilon_c \quad (14)$$

### 2.4 Ultimate strength surface of concrete

The ultimate strength surface of concrete in triaxial stress space is described in this study by the four parameter surface proposed by Hsieh *et al.* (1979) and is expressed as,

$$f(I_1, J_2, \sigma_1) = a\bar{J}_2 + b\sqrt{\bar{J}_2} + c\bar{\sigma}_1 + d\bar{I}_1 - 1 = 0 \quad (15)$$

where,

$$\bar{\sigma}_1 = \frac{\sigma_1}{f_c}, \quad \bar{I}_1 = \frac{(\sigma_1 + \sigma_2 + \sigma_3)}{f_c} \quad (16)$$

$$\bar{J}_2 = \frac{(\sigma_1 - \sigma_2)^2 + (\sigma_2 - \sigma_3)^2 + (\sigma_3 - \sigma_1)^2}{6(f_c)^2} \quad (17)$$

and

$$a = 2.018, \quad b = 0.9714, \quad c = 9.1421, \quad d = 0.2312 \quad (18)$$

From the ultimate surface, the strength enhancement in triaxial state is modeled by modifying the peak stress of the uniaxial stress-strain curve as bellows

$$f_{ci} = \lambda_{si} f_c, \quad f_{fi} = \lambda_{si} f_f \quad (19)$$

where  $\lambda_{si}$  is the strength enhancement factor solved from the equation of ultimate surface. On the other hand, experiments have shown that concrete behaves more ductile for increasing confinement pressure. To account for increasing ductility in high confinement pressure, from experimental results by Kupfer, *et al.* (1969) and Smith (1987), the ductility enhancement is newly proposed as the function of the strength enhancement factor as

$$\lambda_{ei} = 0.3 + 0.7 \lambda_{si}^2, \quad \text{if } \lambda_{si} < 3 \quad (20)$$

$$\lambda_{ei} = 5 \lambda_{si} - 8.4, \quad \text{if } \lambda_{si} \geq 3 \quad (21)$$

where  $\lambda_{ei}$  is the strain enhancement factor, and the enhanced strains corresponding to the peak and

ultimate stresses respectively can be expressed as

$$\epsilon_{ci} = \lambda_{ei}\epsilon_c, \quad \epsilon_{fi} = \lambda_{ei}\epsilon_f \tag{22}$$

### 3. Concrete model in tension

Concrete cracking model is considered as a smeared crack approach. If the maximum principal stress for some reason exceeds a limiting value, a crack is assumed to form in a plane orthogonal to this stress. After this, the behavior of that zone of concrete becomes orthotropic. After cracking, new sets of cracks can be formed which are perpendicular to the previous cracks as shown in Fig. 3.

After concrete cracking, tensile stress is not immediately released to zero but is gradually released by strain-softening behavior. In this paper, as proposed by Yamaguchi *et al.* (1990), after concrete cracking, the stress-strain relation is considered as a linear strain-softening model. As shown in Fig. 4, the total strain increment  $\Delta\epsilon$  is decomposed into two parts, the concrete strain increment  $\Delta\epsilon_{co}$  and the crack strain increment  $\Delta\epsilon_{cr}$ , and the strain-softening modulus  $E_t$  can be derived as follows,

$$\frac{1}{E_t} = \frac{1}{E_o} + \frac{1}{C_{cr}}, \quad C_{cr} = -\frac{f_t^2 w_f}{2G_f} \tag{23),(24)}$$

where  $G_f$  is defined as the fracture energy of concrete required to create one unit of area of a continuous crack and  $w_f$  is the crack band width.

Experimental results indicate that a considerable amount of shear stress can be transferred across the rough surfaces of cracked concrete due to the influences of the aggregate interlocking,

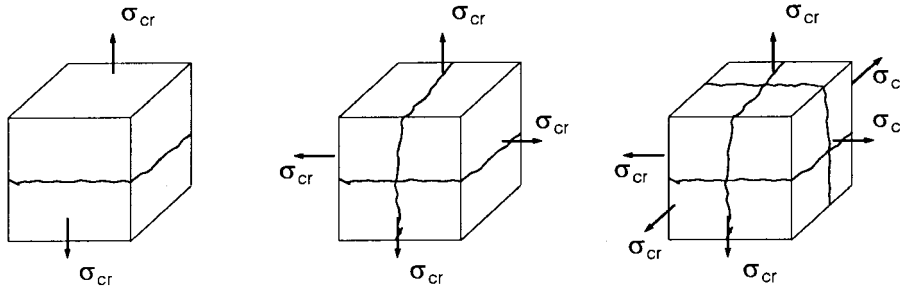


Fig. 3 Three-dimensional crack model

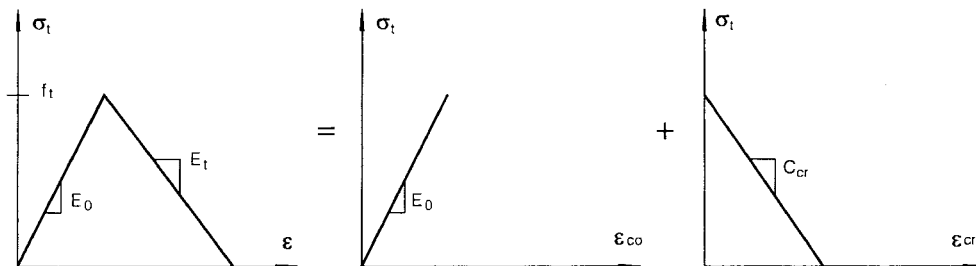


Fig. 4 Linear tensile strain-softening model of concrete

reinforcement ratio and bar size. A common procedure to account for aggregate interlock in a smeared crack model is to attribute an appropriate value to the cracked shear modulus  $G_c$  as a function of the uncracked shear modulus  $G$ . In the present work, from Kolmar *et al.* (1984), if strain exceeds tensile strain  $\epsilon_t$ , the cracked shear modulus are assumed to be reduced linearly as

$$G_c = \alpha_c G \left( 1 - \frac{\epsilon}{\epsilon_m} \right), \quad \text{for } \epsilon_t \leq \epsilon < \epsilon_m \quad (25)$$

where  $\alpha_c$  is used as 0.5 for one crack and 0.25 for over two cracks, and  $\epsilon_m$  is used as 0.002.

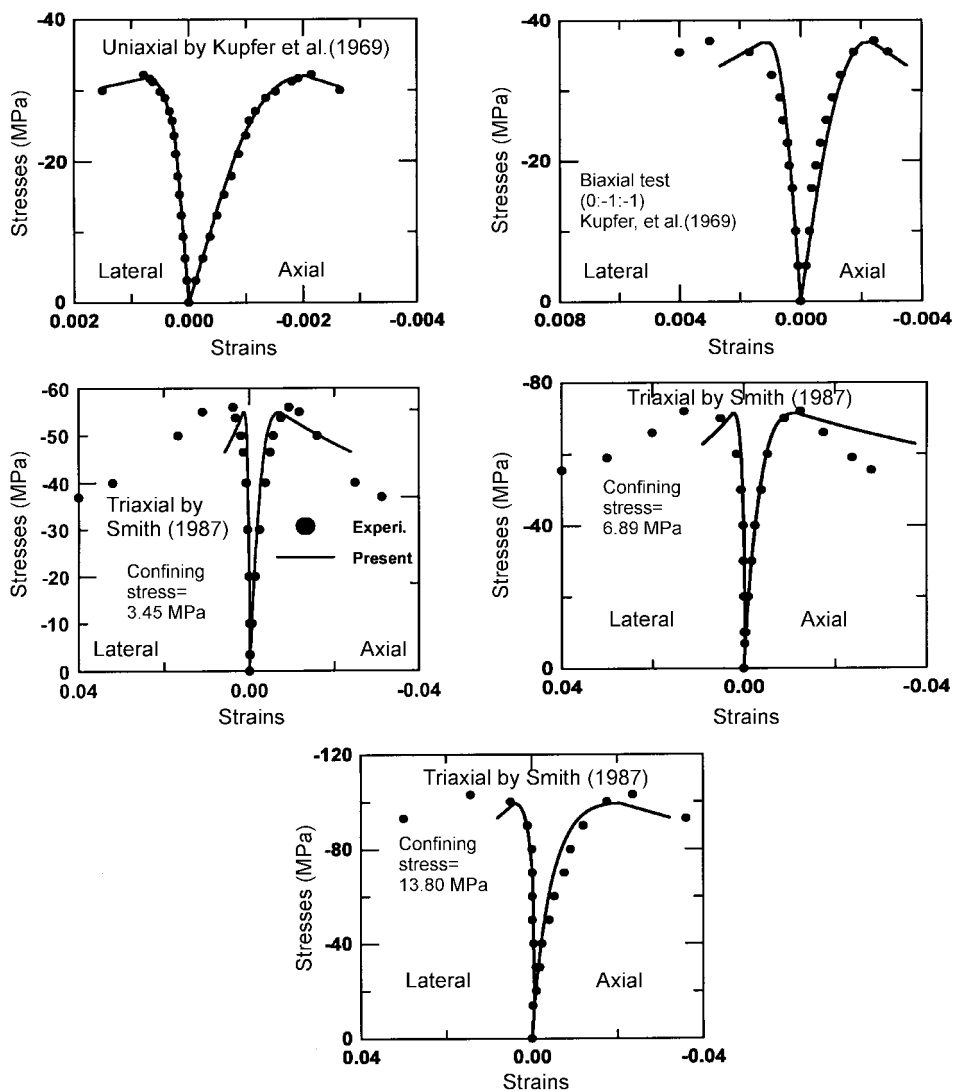


Fig. 5 Uniaxial, biaxial, and triaxial stress-strain curves

#### 4. Comparison with the stress-strain test results

Uniaxial, biaxial and triaxial stress-strain relationships obtained from the foregoing model are compared with the experimental results by Kupfer *et al.* (1969) and Smith (1987) as shown in Fig. 5. The uniaxial compressive strength of concrete is 32MPa for uniaxial and biaxial tests and 34.7 MPa for triaxial tests. As could be seen, the peak compressive stresses from predicted results by present model in all cases had a good agreement with those from the experimental tests, and ductility response in compressive ascending portion is closer to the experimental results. However the response in compressive descending portion is somewhat different from the experimental results.

#### 5. Behavior of steel reinforcement

The reinforcing bar is considered as 2-noded isoparametric bar element to resist only axial force in the bar direction. Isoparametric bar element can be easily matched by placing them on solid elements. A bilinear idealization is adopted in order to model the bilinear elastic and strain-hardening plastic stress-strain relationships. It is assumed that between steel reinforcement and concrete is perfectly bond in the present study. On the other hand, in the case of tensile steel embedded in concrete, since the steel stress remains lower than the yield strength everywhere else besides the vicinity of the crack plane, the average strain of the bar does not exhibit a yield shelf as does a bare bar. The strain-hardening rate is dependant on the average steel stress at the start of yielding, and is higher when the stress is lower. In present model, in order to model the post-yielding constitutive laws for a bar embedded in concrete, the average stress and average strain relationship proposed by Okamura and Maekawa (1991) is considered.

#### 6. Analysis of reinforced concrete beams

Based on the detailed descriptions in the previous sections, a three-dimensional finite element program for reinforced concrete structures, NFERC4P, is developed. The 8-noded hexahedral elements are used to model concrete solids. The nonlinear problem is solved by the modified Newton-Raphson approach. The tangential stiffness matrix is recalculated for each load increment or when the concrete newly cracks. Convergence criteria in terms of incremental nodal displacements are adopted in order to terminate the iterative cycle when the solution is considered to be sufficiently accurate. In order to investigate the compressive strength of concrete in the flexural region of reinforced concrete structural members, a simple beam and a structural beam member connected with beam-column joint are taken as numerical examples in the following sections.

##### 6.1 RC simple beam

An example model for reinforced concrete simple beam subjected to 4-point transverse load experimentally tested by Kotsovovs, *et al.* (1982) is analyzed. It was known that the experiment determined failure due to the flexural crushing of concrete near the top of the middle of the beam. The geometry, reinforcement details and its finite element mesh are illustrated in Fig. 6. Taking

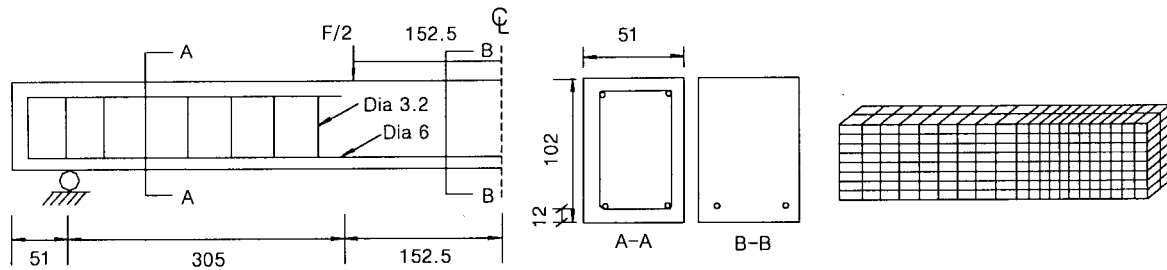


Fig. 6 Analysis model of RC simple beam

advantage of the symmetry, only half of the specimen is used in the analysis. This beam has tensile and compressive longitudinal reinforcements and transverse shear reinforcement, but no compressive and shear reinforcements between two load points.

Material properties of concrete are assumed to be as follows; uniaxial compressive strength  $f'_c$  of 37.8 MPa and its corresponding strain  $\epsilon_c$  of 0.002, uniaxial tensile strength  $f_t$  of 3.78 MPa, ultimate strain  $\epsilon_f$  of  $4\epsilon_c$ ,  $k_f$  of 0.75, initial Young's modulus  $E_o$  of 29,000 MPa, initial Poisson's ratio  $\nu_o$  of 0.19,  $G_f$  of 180 N/m,  $w_f$  of 15 mm. Properties of reinforcing bars are as follows; yield stress  $f_y$  of 417 MPa, Young's modulus  $E_s$  of 200,000 MPa, modulus of strain-hardening  $E_{sh}$  of 2,000 MPa, diameter of 6.0 mm for tensile and compressive longitudinal bars and 3.2 mm for transverse reinforcements.

From numerical analysis, the load-displacement relation at center is presented in Fig. 7, comparing with the experimental results. Although the yielding point of steel reinforcement is slightly higher than the experimental value, the nonlinear behavior of present model gives very similar result to the experimental result.

Fig. 8 shows the cracked patterns observed in the experimental test and predicted in the finite element analysis at failure load. The crack pattern predicted in the present analysis has the same tendency as the experimental results that flexural cracking is dominant near the mid-span of specimen. Both numerical and experimental results show that the flexural failure is the predominant failure pattern. Longitudinal tensile steel bar is yielded and its maximum strain is 0.0056, but

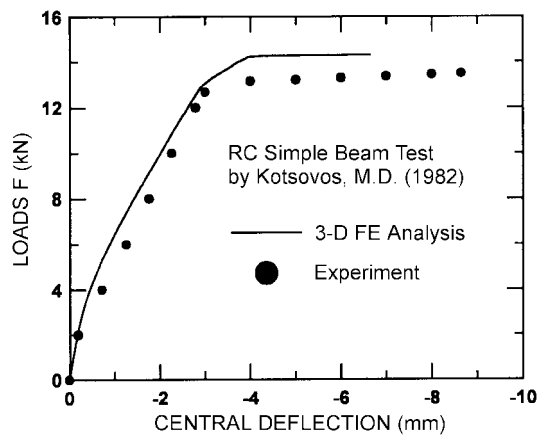


Fig. 7 Load-displacement at center

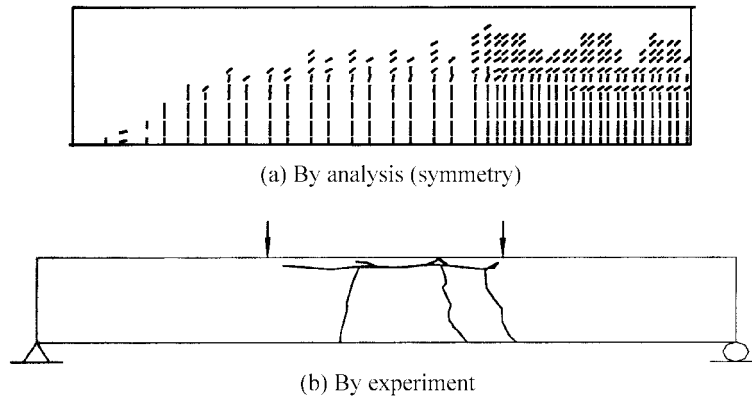


Fig. 8 Crack distributions at failure

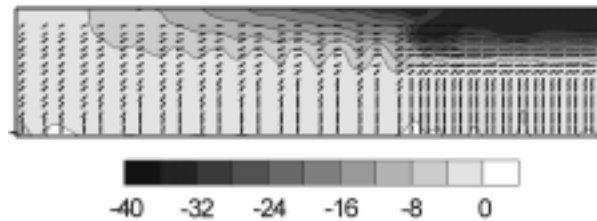


Fig. 9 Contour of principal compressive stress (MPa)

longitudinal compressive and transverse reinforcements are not yielded.

Fig. 9 shows the contour of principal compressive stress and its direction on outer surface of specimen at failure load. It can be seen from the stress contour, the elements at top and bottom near the mid-span of specimen are subjected to compression and tension, respectively. However, the severely loaded region exists at top between two loading points. The first crushing point of concrete, so called the critical section by flexural compressive failure, appears at the cross-section of 129.8 mm away from the central section of beam. The peak value of principal compressive stress in the vicinity of critical section is observed similar with the value of the uniaxial compressive strength of concrete, except from the loading points.

Fig. 10 shows the distribution of cross-sectional stresses both at central and critical sections. These stresses mean member directional stresses obtained from the average of stresses at Gauss point about beam width. Both at central and critical sections, the distributions of cross-sectional stresses are similar with the uniaxial stress-strain curve of concrete.

### 6.2 RC beam member connected with beam-column joint

Another example model for reinforced concrete structural beam member connected with beam-column joint at center is considered. This beam has two longitudinal tensile reinforcing bars, but no longitudinal compressive and transverse shear reinforcements. The geometry, reinforcement detail and its finite element mesh are illustrated in Fig. 11. The experiment of this beam member was conducted at the University of Illinois and had been reported by Burns, *et al.* (1966). This beam is

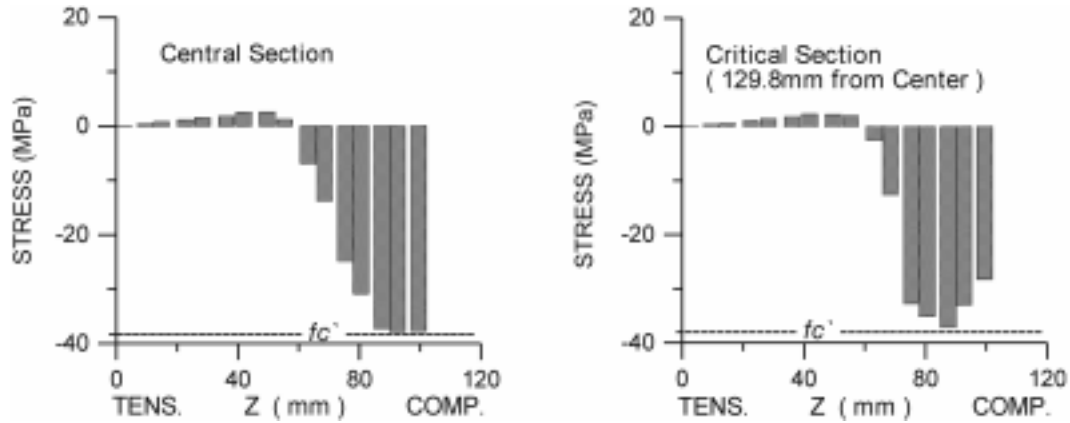


Fig. 10 Concrete stresses at cross-section

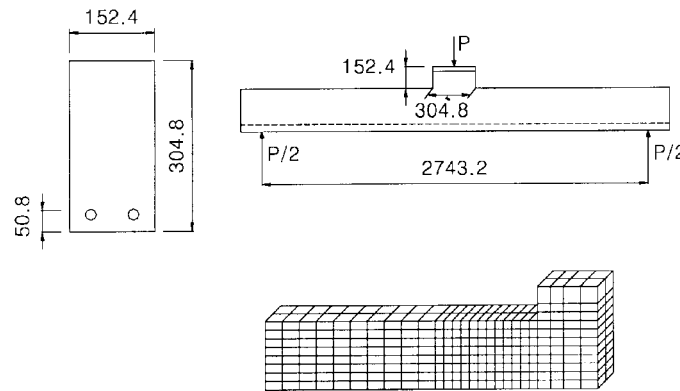


Fig. 11 Finite element model of RC structural beam member (Burns, *et al.* 1966)

152.4 mm by 304.8 mm (6 inch by 12 inch) in cross section, with a span between simple supports of 2743 mm (9 ft). This experiment was conducted to obtain a better understanding of the load-deflection behavior of reinforced concrete beam members loaded to failure, particularly the plastic hinging that develops at the connection of a beam to a column in a frame.

Considering the symmetry of the loading, boundary, and geometric conditions, only half of the specimen is considered in the present analysis model.

Based on the experimental data, material properties of concrete are assumed to be as follows; uniaxial compressive strength  $f'_c$  of 18.2 MPa and its corresponding strain  $\epsilon_c$  of 0.002, uniaxial tensile strength  $f_t$  of 1.82 MPa, ultimate strain  $\epsilon_f$  of  $4\epsilon_c$ ,  $k_f$  of 0.75, initial Young's modulus  $E_o$  of 21,000 MPa, initial Poisson's ratio  $\nu_o$  of 0.19,  $G_f$  of 180 N/m,  $w_f$  of 15 mm. Properties of tensile reinforcing bars are as follows; yield stress  $f_y$  of 310 MPa, Young's modulus  $E_s$  of 155,000 MPa, strain-hardening modulus  $E_{sh}$  of 2,700 MPa, diameter of 13.0 mm.

Beam failure in the experiment followed the formation of plastic hinge, which resulted from the crushing of concrete at top fiber near the connection of the beam and the column in a frame. The transverse load-deflection responses both in experiment and the present analysis are illustrated in Fig. 12. In the experiment, the ultimate load carrying capacity was 40.1 kN at the mid span

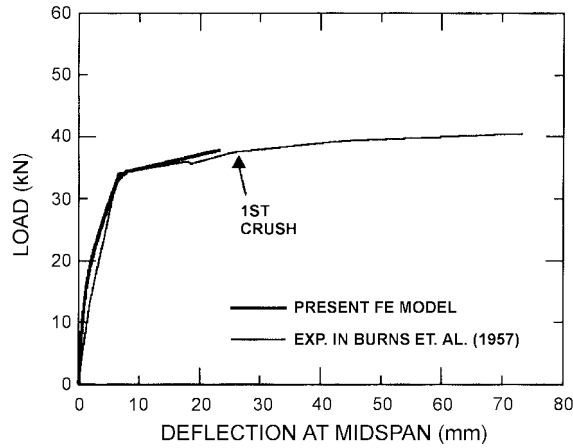


Fig. 12 Load-deflection response

deflection of 7.3 cm, the first crushing point, however, was at the load level of 37.8 kN at the mid span deflection of 2.6 cm. From the results of numerical analysis, the specimen is failed by the formation of plastic hinge resulted from the first crushing of concrete in the vicinity of beam-column connection. The analysis has been stopped at this point. The analysis result of load-deflection response is very close to the experimental observation when the test reaches the first crushing point of concrete as shown in the figure. The longitudinal tensile reinforcement is yielded and the maximum tensile strain reaches to 0.0032 at the load level of the first crushing.

Fig. 13 illustrates the cracked patterns predicted in the present analysis at two load levels. The predicted crack pattern has the tendency that flexural bending cracking is dominant in the vicinity of the mid-span.

The distribution of principal compressive stresses and their directions on outer surface of specimen at the crushing of concrete are illustrated as shown in Fig. 14. It can be seen from the stress contour, concrete at top fibers in the vicinity of beam-column joint is under severely

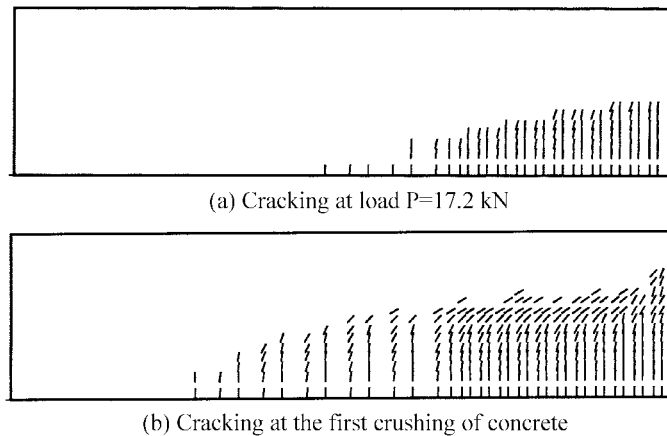


Fig. 13 Crack distributions by the present analysis

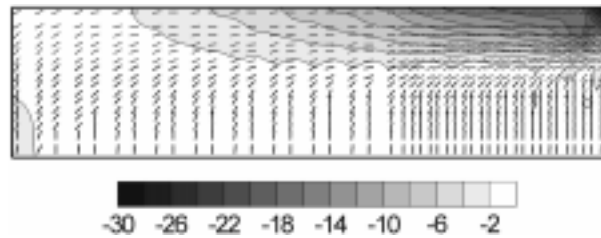


Fig. 14 Contour of principal compressive stresses (MPa)

compressive stress state. The principal compressive stresses in the region highly exceed the value of the uniaxial compressive strength of concrete. The first crushing point of concrete, so called the critical cross-section by the failure of concrete crushing, is located at the cross-section of 42.3 mm away from the beam-column joint connection. It is because the compressive concrete near the top fibers of each cross section in the vicinity of the beam-column joint connection is not simply a uniaxial compressive state. Table 1 illustrates the three relative principal stresses  $\sigma_i/f_c'$  and their corresponding principal strains at top fibers of three cross-sections. It shows that the concrete at top fiber of the first two cross-sections from beam-column joint is under the triaxial compressive stress state, however, the concrete at top fiber of the critical cross-section is under the biaxial compressive stress state.

Fig. 15 illustrates the distribution of the cross-sectional concrete stresses both at joint and critical cross-sections. At joint cross-section, the peak compressive stress of concrete exceeds the uniaxial

Table 1 Relative principal stresses and the corresponding strains at top fibers

Location from joint	Relative principal stresses	Corresponding principal strains
0.0 mm (joint section)	(-0.16, -0.34, -1.62)	(-0.00016, -0.00038, -0.00232)
27.6 mm	(-0.16, -0.27, -1.46)	(-0.00015, -0.00028, -0.00219)
42.3 mm (critical section)	(0.01, -0.02, -0.75)	(0.00005, -0.00002, -0.0081)

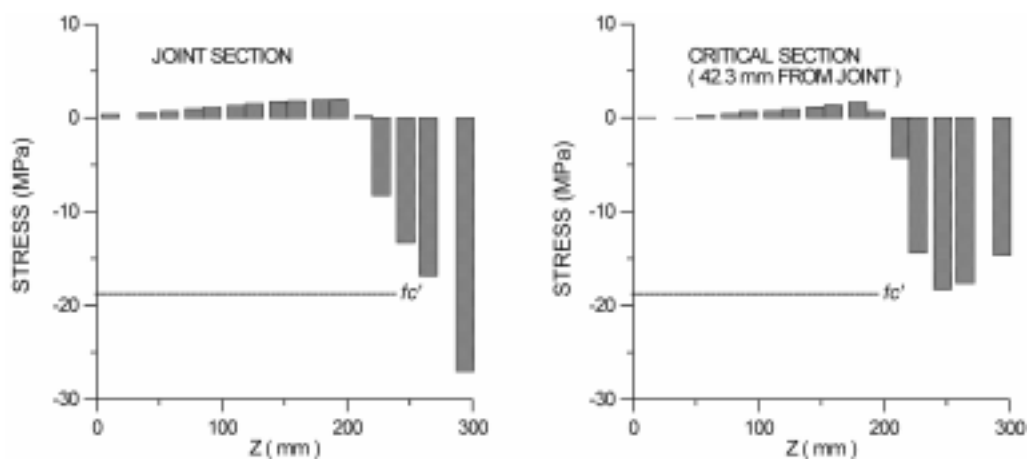


Fig. 15 Cross-sectional concrete stresses

compressive strength of concrete, and the distribution of the cross-sectional concrete stress is not matched with the uniaxial stress-strain curve of concrete. The stress state of concrete near the top fibers of cross-section between the beam-column joint and the critical cross-section becomes a triaxial compressive stress state. The critical cross-section by crushing of concrete is away from the cross-section of the beam-column joint as the distance of 43.2mm, which causes the actual bending span length of the beam to be shorter.

The compressive strength of concrete in reinforced concrete structural member, in general, is considered as the uniaxial compressive strength obtained from cylinder test. Using the three-dimensional finite element model with triaxial stress-strain constitutive law of concrete, reinforced concrete simple beam and structural beam member with beam-column connection were analyzed. From the results of presented analyses, it has known that the concrete in the compression fiber of the cross-section around beam-column joint is not merely under a uniaxial compressive stress state but under a multiaxial compressive stress state. It is because concrete in that region is confined by the existence of beam-column joint, and the region in the vicinity of beam-column joint is commonly the flexural critical cross-section of reinforced concrete beam and beam-column members in a frame. In current design requirements for structural concrete, in the inelastic models for reinforced concrete beam or beam-column elements, the confined stress-strain relationship of concrete has been dealt with the transverse reinforcement or with the steel tube in steel-concrete composite cross-section, but has not been dealt with the influence of the beam-column joint. In actually, it gives consequently a conservative results to predict the flexural bending strength of reinforced concrete structural beam members for regions of greater concrete confinement at the beam-column joint in a frame, as shown in the present example. The phenomena, however, could not be seen in the case of simple beam without a stub to simulate a beam-column joint as shown in Fig. 6.

## **7. Conclusions**

With the development of a three-dimensional finite element formulation implementing the concept of a triaxial constitutive law of concrete based on the recently proposed orthotropic hypoelasticity model, the validation studies have been presented in this paper focused on the triaxial compressive stress-strain relationships of concrete and on the response of reinforced concrete beams in flexural failure. The numerical results show good agreement with the given experiments for the stress-strain relationships of concrete in uniaxial, biaxial, and triaxial compressive tests. In two finite element analyses for a simple beam and a structural beam member, which are failed by concrete crushing in compression, this model closely traces the experimental results in load-carrying capacities, failure mechanisms, yielding of steel, and cracking patterns.

Using the recently developed finite element model, the compressive strength of concrete in flexural regions of reinforced concrete beams has been investigated. In the case of a simple beam, concrete at compression fibers in the vicinity of the flexural critical regions behaves dominant by the uniaxial compressive stress state. In the case of a structural member, however, concrete at compression fibers in the vicinity of the beam-column joint does not dominant by the uniaxial compressive state but does by the biaxial and triaxial compressive stress states. The reason is that the flexural critical cross-section of reinforced concrete structural beam exists at the beam-column joint. The concrete in compression fibers in the region behaves as the confined concrete by the

influence of beam-column joint. In that region, the compressive strength of concrete is not merely in the meaning of a uniaxial compressive strength but a biaxial or a triaxial compressive strength.

This gives a different concept to compare with the present idea for cross-sectional strength of reinforced concrete structural members, as presented in ACI code requirements for structural concrete (1999), in the models for cross-sectional analysis using the equivalent rectangular stress block theory (Hognestad, *et al.* 1955), or in the fiber model (Kaba, *et al.* 1984), in which the compressive stress-strain curve of concrete at flexural critical cross-section is considered as a uniaxial compressive stress-strain curve of concrete. This idea underestimates the compressive strength of concrete in actual concrete structural beam members in a frame. For the reason of the severe confinement of concrete at the beam-column joint, the flexural critical cross-section is observed at a small distance away from the beam-column joint, and the actual flexural span length of the member has become shorter than the real span length of the member. These observations should be made that there will be actually economies in design practice for structural beam members in a frame resulting from concrete confinement due to the influence of the beam-column joint.

In this paper, concrete confinement and its effects on the flexural strength of reinforced concrete beam member in the vicinity of beam-column joint have been studied mainly based on the observation of numerical results, with limiting to the case of no transverse shear reinforcement. Since the triaxial stress of concrete in member test does not able to be measured directly through experiment, this research is mainly focus on the numerical observations. The results of the recent study point to future enhancements, such as the study with more abundant observations of experimental results with developing the method for the measurement of triaxial stresses of concrete in member tests, the study with the case of transverse shear reinforcement, and the study on reinforced concrete beam-column members loaded both on the uniaxial and biaxial bending.

## References

- ACI Committee 318 (1999), *Building Code Requirements for Structural Concrete (ACI 318-99) and Commentary (318R-99)*, American Concrete Institute, Farmington Hills, Mich.
- Burns, N.H., and Siess, C.P. (1966), "Plastic hinging in reinforced concrete," *J. Struct. Eng. Div. ASCE*, **92**(ST5), October, 45-64.
- Darwin, D., and Pecknold, D.A. (1977), "Nonlinear biaxial law for concrete," *J. Eng. Mech. Div. ASCE*, **103**(EM2), 229-241, April.
- Elwi, A.A., and Murray, D.W. (1979), "A 3D hypoelastic concrete constitutive relationship," *J. Eng. Mech. Div. ASCE*, **105**(EM4), 623-641.
- Hognestad, E., Hanson, N.W., and McHenry, D. (1955), "Concrete stress distribution in ultimate strength design," *J. of ACI*, **52**(6), 455-479.
- Hotta, H., and Cho, C.G. (1999), "Three-dimensional finite element analysis on compressive strength of concrete prisms with several height/width ratios," *J. Struct. Constr. Eng., Architectural Institute of Japan*, 517.
- Hsieh, S.S., Ting, E.C., and Chen, W.F. (1979), "An elastic-fracture model for concrete," *Proc. 3d Eng. Mech. Div. Spec. Conf. ASCE*, 437-440, Austin, Texas.
- Kaba, S.K., and Mahin, S.A. (1984), "Refined modeling of reinforced concrete columns for seismic analysis," Earthquake Engineering Research Center, Univ. of California, Berkeley, Report No. UCB/EERC-84/03.
- Kolmar, W., and Mehlhorn, G. (1984), "Comparison of shear formulations for cracked reinforced concrete elements," *Proc. of the Int. Conf. on Comp. Aided Analysis and Design of Conc. Struc.*, Part I, Pineridge Press, Swanses, U. K., 133-147.

- Kotsovos, M.D. (1982), "A fundamental explanation of the behavior of reinforced concrete beams in flexural based on the properties of concrete under multiaxial stress." *Mat. & Struct., RILEM*, **15**, 529-537.
- Kupfer, H.B. and Gerstle, K.H. (1973), "Behavior of concrete under biaxial stresses," *J. of Eng. Mech. Div., ASCE*, **99**(4), 852-866.
- Kupfer, H.B., Hildorf, H.K., and Rusch, H. (1969), "Behavior of concrete under biaxial stresses," *J. of ACI*, **66**(8), 656-666.
- Okamura, H., and Maekawa, K. (1991), *Nonlinear Analysis and Constitutive Models of Reinforced Concrete*, Gihodo.
- Saenz, L.P. (1964), "Discussion of equation for the stress-strain curve of concrete by Desayi and Krishman," *J. of ACI*, **61**, 1229-1235, September.
- Smith, S.H. (1987), *SRS Report, 87-12*, Dept. of Civ. Arch. and Env. Eng., Univ. of Colorado, Boulder.
- Takiguchi, K., and Hotta, H., Mizobuchi, T., and Morita, S. (1992), "Fundamental experiments on compressive properties of concrete around the critical section of R/C column," *J. Struct. Constr. Eng., Architectural Institute of Japan*, **442**, December, 111-122 (in Japanese).
- Takiguchi, K., Imai, K., and Mizobuchi, T. (1997), "Compressive strength of concrete around critical section of R/C column under compression-bending-shear," *J. Struct. Constr. Eng., Architectural Institute of Japan*, **496**, June, 83-90 (in Japanese).
- Takiguchi, K., and Miyazaki, Y., and Mizobuchi, T. (1995), "Compressive properties of concrete around critical section of R/C column under antisymmetric eccentric compression," *J. Struct. Constr. Eng., Architectural Institute of Japan*, **478**, December, 143-151 (in Japanese).
- Takiguchi, K., and Morita, S. (1994), "Compressive behaviors of concrete in R/C members subjected to eccentric compression," *J. Struct. Constr. Eng., Architectural Institute of Japan*, **464**, October, 109-118 (in Japanese).
- Yamaguchi, E., and Chen, W.F. (1990), "Cracking model for finite element analysis of concrete materials," *J. Eng. Mech. Div. ASCE*, **116**(6), June, 1242-1260.